

Potential of weather radar in estimating volcanic eruption source parameters: case study of Eyjafjallajökull volcano eruption

L. Mereu^{1,2}, F.S. Marzano^{1,2}, M. Montopoli^{1,2}, C. Bonadonna³

¹DIET, University of Rome, 00184 Rome, Italy

²CETEMPS, University of L'Aquila, 67100 L'Aquila, Italy

³University of Geneva, Switzerland

(Dated: 15 July 2014)



Luigi Mereu

1 Introduction

The Eyjafjallajökull volcano is a high-latitude stratovolcano on the south coast of Iceland, with a summit at 1666 m above sea level (Siebert and Simkin, 2002-2012). The explosive phases of the Eyjafjallajökull eruption began on April 14th, 2010. This activity continued until 18th April (the first explosive phase) and between 18th April and 4th May the eruption intensity felled. The explosive activity resumed on 5th May 2010 and continued with a varying intensity until May 18 (the second explosive phase) (Gudmundsson, 2011) producing fine-grained ash rich plumes. From May 18th the eruption intensity declined, with continuous activity ending on May 22th 2010. Some of the fine-grained ash, produced predominately during the first explosive phase and the early part of the second explosive phase (May 5th-7th, 2010) (Stevenson et al., 2012), was carried over large distances by northwesterly atmospheric winds (Bonadonna et al., 2011; Stevenson et al., 2012; Woodhouse et al., 2013; Bonadonna et al., 2003; Pouget et al., 2013).

The ash dispersal from an explosive eruption is a function of multiple factors, including magma mass flow rate (MFR), degree of magma fragmentation, vent geometry, plume height, particle size distribution and wind velocity (Taddeucci, 2011; Spark, 1997). MFR can then be derived by dividing the erupted mass by the eruption duration (if known) or based on empirical and analytical relations with plume height (e.g. Degruyter and Bonadonna, 2012; Mastin et al., 2009; Woodhouse et al., 2013). By combining data from ground surveys and remote sensing measurements, it is possible to gain more insights into tephra dispersal. In particular, multi-spectral visible and infrared observations from both low-Earth orbit (LEO) and Geosynchronous Earth orbit (GEO) satellites can provide estimates of dispersed fine ash especially over ocean at hundreds of kilometers far away from the vent (Schneider et al., 2012) However, contamination by water clouds, water vapor variability and low sensitivity to particles larger than 10 microns are still open issues for quantitative retrieval.

Microwave radars can be exploited to extract ash spatial-temporal distribution in proximity of the volcano vent (Lacasse et al., 2004; Marzano et al., 2006; Marzano et al., 2011). Radar technology is well established and can nowadays provide fast three-dimensional (3D) scanning antennas together with Doppler and dual polarization capabilities (Marzano et al., 2012). Radar data can be quantitatively interpreted by applying the Volcanic Ash Radar Retrieval (VARR) physically-based technique (Marzano et al., 2006). Previous studies have shown that coarse ash grain sizes larger than 100 microns can be detected by C-band radars at few hundreds of kilometers with a spatial resolution of few kilometers, whereas X-band radars can even detect fine ash particles at closer ranges less than 75 kilometers (Marzano et al., 2012).

The source mass flow of volcanic plume is fundamentally related to the plume height as result of the dynamics of buoyant plume rise in the atmosphere (Morton et al., 1956). Estimates of source mass flow from empirical relationship with the observed rise height can take explicit account of the state of the atmosphere at time of the eruption (e.g., Degruyter and Bonadonna, 2012). This work shows a tentative for estimating ash concentration, mean ash diameters, plume height and mass flow rate from the C-band weather radar observations in Keflavik of the Eyjafjallajökull eruption in 2010. Models and infrasound detections are used as well to make comparisons with the radar estimates. The outcome of this research might be of some utility for the initialization of ash dispersion models thus hopefully improving their forecast skills.

The paper is organized as follows. Section 2 provides an overview of the main ash parameters derived from weather radar and MFR estimation methodologies, Section 3 is dedicated to illustrate MFR and plume top height inter-comparisons, whereas conclusions are drawn in Section 4.

2 Estimation of volcanic eruption source parameters

2.1 Radar-based measurements and retrievals

Meteorological microwave radars can be used to quantitatively estimate the geophysical properties of a volcanic ash cloud, as successfully demonstrated in the last decade (Lacasse et al., 2004; Marzano et al., 2006; Marzano et al., 2011). Under the assumption of Rayleigh scattering, the co-polar horizontally polarized reflectivity factor Z_H ($\text{mm}^6 \text{m}^{-3}$ or dBZ) is related to size distribution of ash particle polydispersion by:

$$Z_H(\tau, \vartheta, \varphi) = \int_{D_1}^{D_2} D^6 N_a(D) dD \quad (2.1)$$

where D (mm) is the equi-volume spherical particle diameter and $N_a(D)$ is the particle size distribution (PSD, in $\text{m}^{-3} \text{mm}^{-1}$) with D_1 and D_2 the expected minimum and maximum particle diameter. A general scaled form has been assumed in previous works to describe ash PSD ($\text{m}^{-3} \text{mm}^{-1}$), formally expressed by (Marzano et al., 2006; Marzano et al., 2010). In this work we have used a PSD reduced to a scaled Gamma function:

$$N_a(D; \mu, \nu, D_n, C_a) = N_n \left(\frac{D}{D_n} \right)^\mu e^{-\Lambda_n \left(\frac{D}{D_n} \right)^\nu} \quad (2.2)$$

where D_n (mm) is the *number-weighted mean diameter*, and in a logarithmic plane, N_n is the intercept, Λ_n is the slope, μ is the shape factor, and ν is the slope factor. The PSD normalization is such that N_n and Λ_n are related to the mean diameter D_n and ash concentration C_a .

If ρ_a (in grams per cubic meter) is the ash density and $m_a = \rho_a (\pi/6) \cdot D^3$ is the mass of sphere-equivalent ash particles, then the *mass concentration* C_a ($\text{g} \cdot \text{m}^{-3}$) can be expressed by:

$$C_a = 10^{-3} \int_{D_1}^{D_2} m_a(D) N_a(D) dD = \frac{\pi}{6} \rho_a m_3 \quad (2.3)$$

where the factor 10^{-3} in (2.3) comes from a dimensional analysis of C_a , D and N_a .

The VARR approach, widely described in previous works (Marzano et al., 2006; Marzano et al., 2010) consists of two main steps: ash classification and ash estimation. Both steps are trained by a physical electromagnetic forward model, basically summarized by (2.1), where the main PSD parameters are supposed to be constrained random variables. Each ash class is characterized by an average effective diameter $\langle D_n \rangle$ and an average concentration $\langle C_a \rangle$. The number of classes N_c is put equal to 9 (3 size classes by 3 mass classes) and each class is supposed to follow a Gaussian random distribution, as shown in previous works (Marzano et al., 2010; Marzano et al., 2011). The ash classification is performed by using the Maximum A Posteriori Probability (MAP) criterion. The probability density function (PDF) of each ash class (c), conditioned to the measured reflectivity factor Z_{Hm} , can be expressed through the Bayes theorem (Marzano et al., 2006; Marzano et al., 2010). For each radar volume bin V_b , the ash concentration C_a ($\text{g} \cdot \text{m}^{-3}$) can be theoretically expressed by means of the ash mass particle m_a . The inversion problem to retrieve C_a from Z_{Hm} can be statistically approached to take into account the inherent parameter variability. Through the training forward model, a power-law regressive approximation may be used as a function of the ash class c -th for estimate C_a for a given volume bin within the 3D radar scan (Marzano et al., 2006; Marzano et al., 2010):

$$\hat{C}_a^{(c)} = a_c Z_{Hm}^{b_c} \quad (2.4)$$

where Z_{Hm} is the measured reflectivity factor and a_c and b_c are the regression coefficients, derived from simulated training dataset for each class c .

Within the usual approximation of Rayleigh backscattering, from the measured radar reflectivity factor Z_{Hm} and the estimated concentration value C_a for a given volume bin, if the class shape parameter $\mu^{(c)}$ is assumed to be constant, it is possible to estimate the mean diameter $D_n^{(c)}$ of the particle distribution through:

$$\hat{D}_n^{(c)} = \sqrt[3]{\frac{Z_{Hm} \rho_a}{f_z(\mu^{(c)}) \hat{C}_a^{(c)}}} \quad (2.5)$$

The erupted mass in the column above the vent can be retrieved by summing the ash concentration of all radar bins in the (radar visible) column itself V_C at a given time step.

The 3D radar-based ash concentration estimate around the volcanic vent can be used to provide an approximate quantification of the MFR. The mass continuity equation states that time variation of the ash mass concentration C_a ($\text{kg} \cdot \text{m}^{-3}$) within a volume above the vent is equal to an input source term, due to the (positive defined) concentration flow rate f_R ($\text{kg} \cdot \text{m}^{-3} \cdot \text{s}^{-1}$), minus a sink term, due to the flow divergence rate, outward the eruption column (Sparks et al., 1997). We can take into account possible air entrainment into the plume (which would dilute the ash concentration) and the ash flows into the umbrella cloud region due to local turbulent circulation. By integrating over the eruption columnar volume V_C above the vent and using the divergence theorem, we obtain:

$$\int_{V_C} \frac{\partial C_a(\mathbf{r}, t)}{\partial t} dV = - \oint_{S_C} \mathbf{n}_0 \cdot [C_a(\mathbf{r}, t) \mathbf{v}(\mathbf{r}, t)] dV + F_R(t) \quad (2.6)$$

where \mathbf{n}_0 is the normal unit vector belonging to the closed surface S_C surrounding the column volume V_C , $\mathbf{v}(\mathbf{r}, t)$ is the plume velocity vector field, whereas the mass flow rate F_R (kg/s) is defined by:

$$F_R(t) = \int_{V_C} f_R(\mathbf{r}, t) dV = \int_{V_C} \frac{\partial C_a(\mathbf{r}, t)}{\partial t} dV + A_R(t) \quad (2.7)$$

and the derivative mass rate D_R (kg/s) and advection rate A_R (kg/s) by:

$$D_R(t) = \int_{V_c} \frac{\partial C_a(\mathbf{r}, t)}{\partial t} dV; \quad A_R(t) = \oint_{S_c} C_a(\mathbf{r}, t) [\mathbf{n}_0 \cdot \mathbf{v}(\mathbf{r}, t)] dS \quad (2.8)$$

We can now determine the MFR by discretizing equation (2.7) as a function of the weather radar measurements around the volcano vent, and then evaluate MFR at each k -th time step t_k from:

$$F_R(t_k) = D_R(t_k) + A_R(t_k) \quad (2.9)$$

If the 3D vectorial velocity field $\mathbf{v}(\mathbf{r}, t)$ of the divergent advection rate A_R is negligible or, in any case, difficult to estimate with a good confidence, from equation (2.8) we can anyway provide an estimate of the mass flow rate by distinguishing the positive time derivative of C_a from its negative derivative one. This means that we may approximate F_R and A_R by:

$$\begin{cases} F_{Rapp}(t_k) = D_{Rapp}(t_k) \equiv \sum_{i=1}^{N_c} \Delta V_i \left. \frac{\Delta C_{aik}^{(c)}(t_k)}{\Delta t} \right|^{+} \\ A_{Rapp}(t_k) \equiv \sum_{i=1}^{N_c} \Delta V_i \left. \frac{\Delta C_{aik}^{(c)}(t_k)}{\Delta t} \right|^{-} \end{cases} \quad (2.10)$$

where the right-hand side terms indicate the positive (negative) time derivative of the ash concentration C_a within each radar volume bin. The terms A_{Rapp} is practically estimated using the technique described in Montopoli et al., 2012.

Starting from the VARR-estimated C_a , we can derive another important source parameter, i.e. the top plume height using a threshold C_{ath} on estimated C_a as follows:

$$H_{Ca}(r, \vartheta, \varphi; t) = \text{Max}_z [z | C_a((r, \vartheta, \varphi; t) \geq C_{ath})] \quad (2.11)$$

where Max_z is the maximum operator with respect to altitude z (Marzano et al., 2012).

2.2 Mass flow rate estimations from analytical models and infrasonic techniques

The MFR, reconstructed from radar scans directly probing the ash column above the volcano vent, can be compared with that derived from simplified one-dimensional (1D) eruption models (Degruyter and Bonadonna, 2012; Marzano et al., 2006; Sparks, 1986; Peterson et al., 2010). In particular, it is well known that MFR can be related to a power of the plume height top height H_t (Sparks, 1997). Several analytical formulas have been proposed in the last decades; more recently a nonlinear model has been derived including both wind and buoyancy local meteorological conditions at a given instant through (Degruyter and Bonadonna, 2012):

$$F_R(t) = a_0 [a_1 H_t^4(t) + a_2 H_t^3(t)] \quad (2.12)$$

where a_0 , a_1 and a_2 are coefficients dependent on the gravitational acceleration, air density, buoyancy frequency, top-hat profile radial entrainment coefficient, wind entrainment coefficient and wind velocity profile. Inter-comparisons between equations (2.9) and (2.12) are of interest for validation of the 1D analytical model of Degruyter and Bonadonna, 2012 (hereinafter D&B) and consistency check of MFR estimates (Marzano et al., 2012).

The radar-based MFR estimation can be compared with those derived from infrasound techniques (Ripepe et al., 2013). The acoustic signal recorded during the eruption event, can be converted into plume exit velocity. Assuming that the acoustic velocity u of the expanding surface within the conduit is equivalent to the plume exit velocity at the vent, we can derive MFR directly from the acoustic pressure (Ripepe et al., 2013):

$$F_R(t) = 6.768 \rho_p R^{1.66} \left[\langle p \rangle \frac{r \cdot u}{\rho_{air}} \right]^{1/3} \quad (2.13)$$

where ρ_p is the mixture density, ρ_{air} the air density, R the source radius and r the distance at which acoustic pressure is measured.

3 Eyjafjallajökull eruption on May 6th, 2010: intercomparison between sensor retrievals and model estimates

In this section radar-based estimations of MFR and intercomparison with other methodologies will be shown for the time window from 00:00 to 24:00 UTC on May 6th, 2010 during the Eyjafjallajökull volcanic eruption.

Fig. 1 shows in the upper three panels the histogram of mean diameter D_n , calculated at three first elevation angles above volcano vent, showing a D_n value in a logarithmic scale, with a peak around 0.3 mm, then identifying coarse ash class for the three elevation angles; the lower three panels show the ash concentration C_a estimation histogram for the same angles, with several peaks that vary mainly between 0.1 and 2 g·m⁻³, then small and medium concentration.

Fig. 2 presents the time trend of radar-based MFR estimation with the superimposition of MFR derived from the Degruyter-Bonadonna (D&B) model, MFR computed for height estimations using from radio-sounding wind fields and

MFR from infrasound data. In the same figure, the approximate derivative mass rate D_{Rapp} , obtained from D_R setting to zero the negative values, that is the A_R values in (2.9), is also shown. Differences between radar-based MFR and model-based MFR are noted mainly due to different time-space sampling and sensor sensitivity. Anyway, the D&B model-based estimations are of the same order of magnitude with the radar-derived ones.

Fig. 3 shows the superimposition between radar-based and infrasonic-based plume top height estimation where radar retrievals are obtained by imposing a concentration C_a threshold ($10^{-6} \text{ g}\cdot\text{m}^{-3}$) within VARR. An increase of height estimation from 12:00 till 17:00 is noted in both estimations.

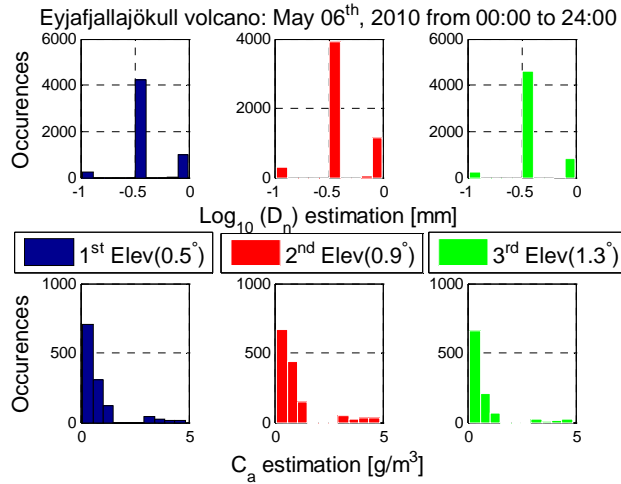


Fig 1: The upper panels show the histograms of VARR-derived mean diameter D_n in logarithmic scale, whereas lower panels show ash concentration C_a for the identified coarse ash classes, estimated around the volcano vent for 24 hours on May 6th, 2010 both for the first three elevation angles above the volcano vent.

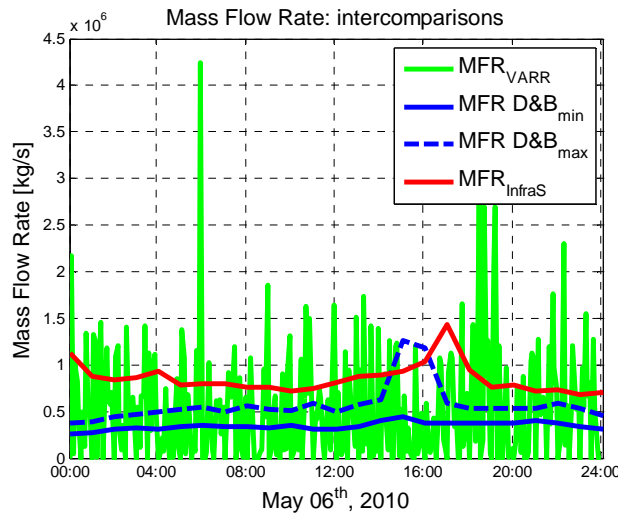


Fig 2: Comparison of temporal trends of VARR-estimated MFR (without the advection term, F_{Rapp}) with 1D model-based MFR, deduced from the Degruyter-Bonadonna (D&B) formula for minimum/maximum plume height estimations and MFR derived from infrasonic retrieval techniques.

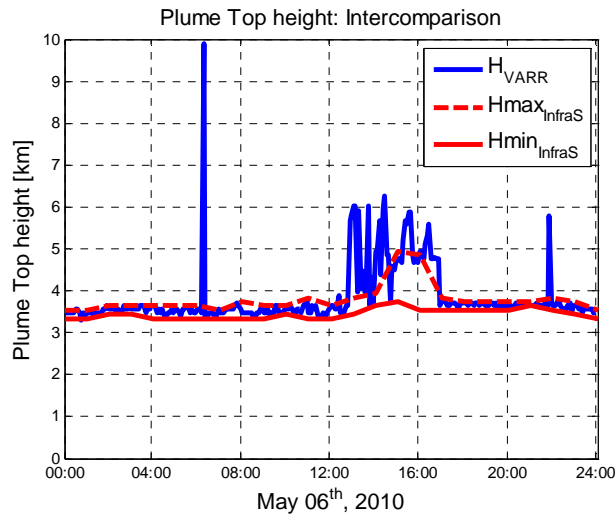


Fig 3: Radar-based estimation of plume top height (H_{VARR} using C_a -threshold technique within VARR) and intercomparisons with minimum and maximum infrasonic array estimation (H_{InfraS}) from 00:00 till 24:00 UTC on May 6th, 2010 during the Eyjafjallajökull volcanic eruption..

When the plume advection velocities term is considered, the correlation among VARR-estimated MFR and model-based MFR, deduced from the D&B model, for different wind speeds (30 and 60 m/s) is shown in the Fig.4.

For May 6th, 2010 the radar-estimated MFR values are around $3 \cdot 10^6$ kg/s. Using the H_{VARR} estimation as an input for the D&B 1D model, the obtained MFR values can vary around 10^6 kg/s consistently with the radar-based values. This result confirms that MFR estimates, derived from C-band radar measurements available every 5 minutes, can provide a valuable information for assessing the volcanic eruption activity.

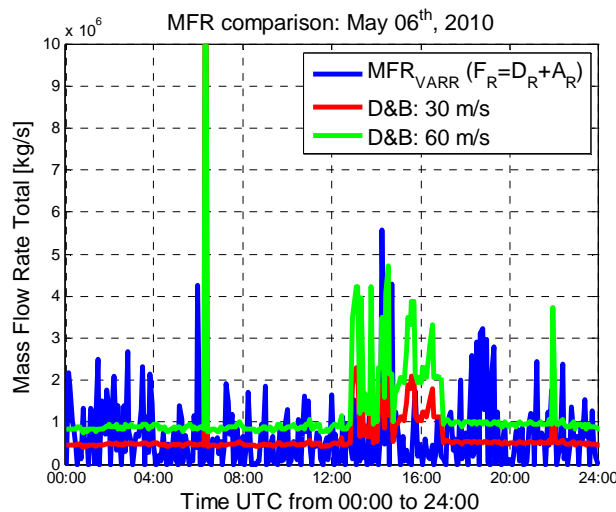


Fig 4: Correlation among VARR-estimated MFR (considering the advection terms, F_R) and model-based MFR, deduced from the Degruyter-Bonadonna 1D formula for different wind speeds (30 and 60 m/s).

4 Conclusions

The extended VARR methodology to estimate MFR starting from microwave radar observables has been shown in this work. Microwave radars can probe the internal structure of the plume, even though they are less sensitive to finer ash grains. The estimate of the volcanic MFR is a crucial goal for eruption dynamics modelling in order to forecast accurately the atmospheric dispersion of ash concentration during volcanic events. To this aim, it is important to know the volcanic source parameters which initialize the transport of ash particles from the volcano to the atmosphere.

The MFR, estimated by means of VARR for whole day of May 6th, 2010, presents a range of values agreeing quite well with those obtained by 1D analytical models and infrasonic array techniques. Indeed, 1D model can underestimate MFR if atmospheric wind effects are neglected. The intercomparison of VARR-based MFR estimations with those derived from infrasonic arrays has further highlighted the coherence of radar algorithm itself.

Future works should be devoted to improve and apply the VARR algorithms to microwave radar data with higher sensitivity and quality, exploiting observations at shorter distances and possible radar polarimetric capability.

Acknowledgement

We are very grateful to B. Pálmason, H. Pétursson and S. Karlsdóttir (IMO, Iceland) for providing C-band radar data and useful suggestions on data processing. We also thank W. Degruyter (University of Geneva, CH) for helpful suggestions and M. Ripepe (University of Florence, Italy) for infrasonic array data provision.

References

- Bonadonna, C., R. Genco, M. Gouhier, M. Pistolesi, R. Cioni, F. Alfano, A. Hoskuldsson and M. Rippe**, Tephra sedimentation during the 2010 Eyjafjallajökull eruption (Iceland) from deposit, radar, and satellite observations. *Journal of Geophysical Research*, vol 116, B12202, 2011.
- Bonadonna, C. and J. C. Phillips**, Sedimentation from strong volcanic plumes, *Journal of Geophysical Research*, vol 108, NO. B7, 2340, 2003.
- Degruyter W. and Bonadonna C.**, Improving on mass flow rate estimates of volcanic eruptions, *Geophysical Research Letters*, vol.39, L16308, 2012.
- Gudmundsson, M.T., T. Thordarson, A. Hoskuldsson, G. Larsen, H. Bjornsson, F. Prata, B. Oddsson, E. Magnusson, Hognadottir T., G. N. Petersen, C. L. Hayward, J. A. Stevenson and I. Jonsdottir**, Ash generation and distribution from the April-May 2010 eruption of Eyjafjallajökull, Iceland., *Nature Scientific Reports*, vol. 2, 572, doi: 10.1038/srep00572, 2012.
- Lacasse, C., S. Karlsdóttir, G. Larsen, H. Soosalu, W. I. Rose, and G. G. J. Ernst**, Weather radar observations of the Hekla 2000 eruption cloud, Iceland. *Bull. Volcanol.*, 66, 5, 457–473, 2004.
- Marzano, F. S., G. Vulpiani and W.I. Rose**, Microphysical characterization of microwave radar reflectivity due to volcanic ash clouds. *IEEE Trans. Geosci. Rem. Sens.*, 44, 313-327, 2006.
- Marzano, F. S., S. Barbieri, G. Vulpiani and W. I. Rose**, Volcanic ash cloud retrieval by ground-based microwave weather radar. *IEEE Trans. Geosci. Rem. Sens.*, 44, 3235-3246, 2006.
- Marzano F.S., S. Marchiotto, C. Textor and D. Schneider**, Model-based Weather Radar Remote Sensing of Explosive Volcanic Ash Eruption, *IEEE Trans. Geosci. Rem. Sensing*, 48, 3591-3607, 2010.
- Marzano, F. S., S. Barbieri, E. Picciotti and S. Karlsdóttir**, Monitoring sub-glacial volcanic eruption using C-band radar imagery. *IEEE Trans. Geosci. Rem. Sensing*, 48, 1, 403-414, 2010.
- Marzano, F. S., M. Lamantea, M. Montopoli, S. Di Fabio and E. Picciotti**, The Eyjafjallajökull explosive volcanic eruption from a microwave weather radar perspective, *Atmos. Chem. Phys.*, 11, 9503-9518, 2011.
- Marzano F.S., M. Lamantea, M. Montopoli, B. Oddsson and M.T. Gudmundsson**, “Validating sub-glacial volcanic eruption using ground-based C-band radar imagery”, *IEEE Trans. Geosci. Rem. Sens.*, ISSN: 0196-2892, vol. 50, pp. 1266-1282, 2012.
- Marzano F.S., E. Picciotti, G. Vulpiani and M. Montopoli**, “Synthetic Signatures of Volcanic Ash Cloud Particles from X-band Dual-Polarization Radar”, *IEEE Trans. Geosci. Rem. Sens.*, vol. 50, pp. 193-211, 2012.
- Marzano, F. S., Scaranari D., Vulpiani G.**, Supervised Fuzzy-Logic Classification of Hydrometeors Using C-Band Weather Radars. *IEEE Trans. Geosci. Rem. Sensing*, Vol. 45, no. 11, 2007.
- Montopoli, M., Marzano, F. S., Picciotti, E., & Vulpiani, G.** Spatially-adaptive advection radar technique for precipitation mosaic nowcasting. *IEEE Journal of Selected Topics in Applied Earth Observations and Remote Sensing*, 5(3), 874-884. Doi: 10.1109/JSTARS.2011.2182506, 2012
- Mastin, L. G. Et al.**, A multidisciplinary effort to assign realistic source parameters to models of volcanic ash-cloud transport and dispersion during eruptions. *J Volcanol. Geoth. Res.* 186, 10-21, 2009.
- Petersen G. N.**, A short meteorological overview of the Eyjafjallajökull eruption 14 April-23 May 2010, *Weather*, 65, 203-207, DOI: 10.1002/wea.634; 2010.
- Pouget S., Bursik M., Webley P., Dehn J., Pavolonis M.**, Estimation of eruption source parameters from Umbrella cloud or downwind plume growth rate. *Journal of Volcanology and geothermal research*, 2013.
- Ripepe M., C. Bonadonna, A. Folch, D.DelleDonne, G.Lacanna, E.Marchetti, A. Hoskuldsson**, Ash-plume dynamics and eruption source parameters by infrasound and thermal imagery: The 2010 Eyjafjallajökull eruption, *Earth and Planetary Science Letters* 366, 2013, 112–121.
- Sauvageot, H.**, Radar meteorology, Artech House, Boston (MA), 1992.
- Sparks, R.**, The dimensions and dynamics of volcanic eruption columns. *Bull. Volcanol.*, 48, 3-15, 1986.
- Sparks, R. S. J., Bursik, M. I., Carey, S. N., Gilbert, J. S., Glaze, L., Sigurdsson, H., and Woods, A.W.**, Volcanic plumes. New York, Wiley, 1997.
- Taddeucci J., Scarlato P., Montanaro C., Cimarelli C., Del Bello E., Freda C.D.**, Aggregation-dominated ash settling from the Eyjafjallajökull volcanic cloud illuminated by field and laboratory high-speed imaging: *Geology*, v. 39, p. 891–894, 2011.
- Yu T., W. I. Rose, and A. J. Prata**, Atmospheric correction for satellite based volcanic ash mapping and retrievals using split-window IR data from GOES and AVHRR, *J. Geophys. Res.*, vol. 107, no. D16, 4311, 2002.

Wilson L., “Explosive volcanic eruptions—II: The atmospheric trajectories of pyroclasts,” *Geophys. J. R. Astron. Soc.*, vol. 30, no. 2, pp. 381–392, 1972

Schneider, D.J., and Hoblitt, R.P., Doppler weather radar observations of the 2009 eruption of Redoubt Volcano, Alaska: *Journal of Volcanology and Geothermal Research*, v. 259, p. 133-144, 2013, doi:10.1016/j.jvolgeores.2012.11.004.

Woodhouse, M. J., A. J. Hogg, J. C. Phillips, and R. S. J. Sparks, Interaction between volcanic plumes and wind during the 2010 Eyjafjallajökull eruption, Iceland, *J. Geophys. Res. Solid Earth*, 118, 92–109, 2013, doi:10.1029/2012JB009592.

Wilson L., “Explosive volcanic eruptions—II: The atmospheric trajectories of pyroclasts,” *Geophys. J. R. Astron. Soc.*, vol. 30, no. 2, pp. 381–392, 1972.